Effects of Powder Reuse and Spatial Location Dependency on the Powder Characteristics and Defect Structure of Additively Manufactured Ti-6Al-4V Parts

Arash Soltani-Tehrani[1,2], Mohammad Salman Yasin[1,2], Shuai Shao[1,2], Nima Shamsaei[1,2,*]

[1]Department of Mechanical Engineering, Auburn University, Auburn, AL, USA
[2]National Center for Additive Manufacturing Excellence (NCAME),
Auburn University, Auburn, AL, USA

[*]Corresponding author:
Email: shamsaei@auburn.edu
Phone: (334) 844 4839

Abstract

In laser powder bed fusion additive manufacturing (L-PBF AM), different powder characteristics including particle size and morphology may yield different packing states and thus different defect content in the resulting parts. As the powder is spread by the recoater, the packing state may not be uniform on the powder bed, giving rise to location-dependent part performance. In addition, as the powder is reused (a common practice in AM industry), its characteristics continuously evolve, causing the defect content to change from build to build. This study aims to investigate the effects of powder reuse and part location on powder characteristics as well as the defect structure of the parts. Results indicate powder reuse in an L-PBF system may reduce the number of defects in the as-fabricated parts due to the superior packing state of reused powder. Part density was also found to be location-dependent, with more defects near the gas outlet.

Keywords: Additive Manufacturing, L-PBF, Powder Recycling, Ti-6Al-4V, Particle Size Distribution (PSD), Location Dependency, Packing State, Powder Flowability

Introduction

Metallic powder is used as the material feedstock in laser powder bed fusion additive manufacturing (L-PBF AM). Therefore, different powder properties can influence the performance of additively manufactured (AMed) parts. For instance, the flowability of non-spherical particles can be inferior due to high inter-particle friction and mechanical interlocking [1–4], and vice versa. As a result, more flowable particles tend to be deposited farther away from the feed bin and the less flowable ones tend to be deposited closer. As a result, a greater location dependency of defect content and mechanical properties are expected for powders with more non-spherical particles [5].

Another powder characteristic that can affect its physical behavior is the particle size distribution (PSD). Fine particles are well known to result in high theoretical powder bed density (PBD) and coarser ones can give rise to higher flowability [6–9]. The reason is that finer particles have typically larger surface-to-volume ratios resulting in higher friction and interlocking [10]. On the other hand, fine particles can fill the voids between coarse particles to give a denser particle arrangement [11].

Powder chemical composition is another critical factor that can affect the final part performance. For instance, the powder can agglomerate with moisture resulting in inferior

flowability and packing state [11], thus higher defect content in the resulting parts. In this condition, inferior mechanical performance such as fatigue resistance and ductility can be expected. During fabrication, the concentration of interstitial elements such as oxygen and nitrogen can also change. The increase of oxygen in Ti-6Al-4V (Ti64) powder has been reported to result in lower ductility and higher material strength [12].

Therefore, powder reuse which can considerably influence the powder characteristics including PSD and particle morphology due to the recycling practice (i.e., top-up or continuously reusing) can be expected to alter the mechanical performance of the AMed parts [13]. In this study, the powder feedstock was continuously reused and the microstructure and defect content of AMed parts were investigated. In addition, parts were placed in four different quadrants to capture any possible location dependency of microstructure and mechanical performance. In the next sections, the experimental program will be provided which will be followed by the experimental results and discussion. Finally, some conclusions will be drawn.

Experimental Program

Plasma-atomized Ti64 Grade 5 powder from AP&C, a GE Additive Company with an initial PSD of 15-53 μm was used as feedstock. After each fabrication, the powder was sieved using an 80-μm mesh and reused for the next iterations. The powder was reused 8 consecutive times without adding any virgin (i.e., unused) powder. It needs to be mentioned that each fabrication was 100 hours giving a total of 800 hours of powder exposure to the fabrication environment. To the authors' knowledge and based on Ref. [13], this is one of the research studies with longest hours of fabrication on the reuse of Ti64 in L-PBF. The same layout was used for all fabrications (see Fig. 1) which consisted of $13 \times 13 \times 97$ and $9 \times 9 \times 83$ mm^3 square blocks to be later machined into fatigue and tensile specimen geometries according to ASTM E466 and E8 [14,15]. The blocks were distributed into four major quadrants, with each quadrant containing some high-strain fracture specimens intended for another study.

The build plate also consisted of some X-ray computed tomography (XCT) coupons (see Fig. 2(a) for the geometry) which were designed to capture the effects of powder reuse and location on the resulting defect content. These coupons were placed in the northeast (NE), north (N), northwest (NW), east (E), center (C), west (W), southeast (SE), south (S), and southwest (SW). two powder containers for PBD measurement (see Fig. 2(b) for the geometry) at different locations were placed in the front (i.e., near to the powder feed bin) and back (i.e., away from the feed bin). Lastly, one microstructure specimen per quadrant was placed on the build plate for further microstructural analyses.

Parts were manufactured using an EOS M290, an L-PBF machine using Ti64 Grade 5 process parameters (Ti64Grade5_040_HiPer). The major infill process parameters were laser power (P) of 280 W, scanning speed (V) of 1300 mm/s, hatching distance (h) of 120 μm, and 40 μm layer thickness (t) resulting in an energy density (E) of 44.87 J/mm^3 (E=P/Vht). Moreover, a laminar flow nozzle was used for fabrication as recommended by the machine manufacturer for processing Ti64 Grade 5. Before each fabrication, the powder was sampled based on ASTM B215 from the feedstock, front, and back locations [16].

In addition, some heat-affected powder was collected from the spatter-rich regions (i.e., near the inert gas outlet as well as the inside and on top of the gas outlet nozzle), as specified in

Ref [17], to track the changes in spatter particles, including their size and population, with continuously reusing the powder. It needs to be specified that all parts were fabricated on 3 mm support structures for convenient removal from the build plate. After fabrication, the XCT and microstructure coupons, as well as the powder containers were removed from the build plate in non-heat-treated (NHT) condition and the remainders of the parts were stress-relieved at 704 °C for 1 hour followed by furnace cooling in an argon environment. The 704 °C SR temperature was selected based on the previous studies on Ti64 [6,7,18,19].
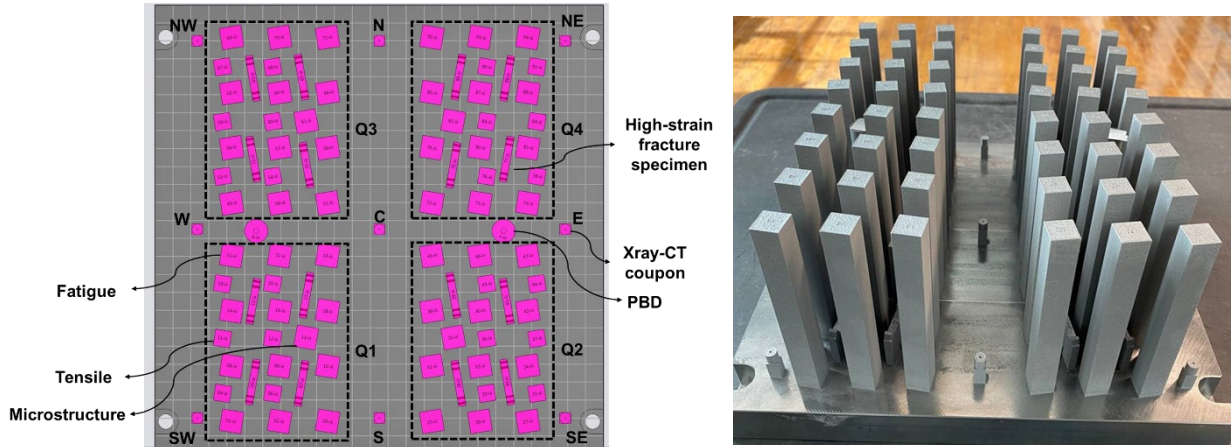

Fig. 1 (a) The top view of the build layout used for fabrication, and (b) parts on the build plate after fabrication.

While the eight times of powder reuse was not significant compared to reuse practices of other practitioners the total time that the powder was exposed to the chamber environment was substantial (100 hours for each built totaling 800 hours) [13]. The XCT coupons were scanned from print 1 (i.e., virgin powder), print 4 (i.e., 3x reused powder), and print 8 (i.e., 7x reused powder) via Zeiss Xradia 620 Versa XCT system to include the first, middle, and last fabrication sets. The imaging conditions were: 4x objective lens, 140 kV voltage, 150 µA current, voxel size 5 µm. To avoid false defect detection, any object detected via intensity thresholding smaller than 10 µm was discarded as defects smaller than 10 µm have usually less probability to result in fatigue failures [20]. The image slices obtained from XCT were then reconstructed using the Zeiss built-in software, and the defects were evaluated using ImageJ.
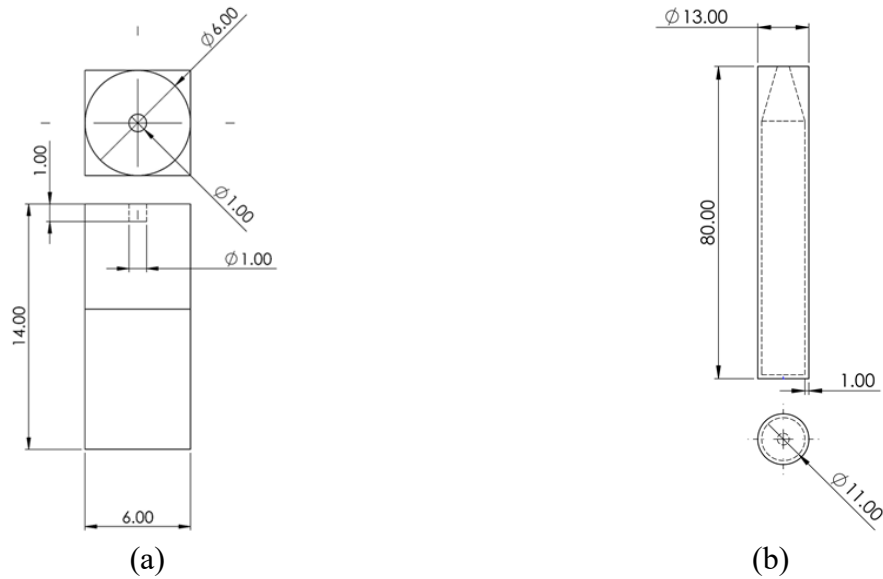
Fig. 2 The geometry of (a) XCT coupons used for defect characterization and (b) powder containers for PBD measurements.

The PBD density was also evaluated with a high-precision scale to capture the weight of the stored powder in the capsules. For powder characterizations, an FT4 powder rheometer was used to obtain powder rheological properties. The analyses included shear stress tests according to ASTM [21] bulk and tapped density tests, and compressibility. Lastly, the morphology and surface chemistry of powder particles were obtained using a Zeiss Crossbeam 550 scanning electron microscope (SEM) and the onboard Oxford energy-dispersive X-ray spectroscopy (EDS) detector. Finally, the hardness for the half-built specimens was measured using a Rockwell C-scale indenter (at 150 kg) with LECO LCR 500. The tests were repeated at least 3 times per condition.

Results and Discussion

The scanning electron microscopy images of particle morphology were obtained for the virgin, 3x-, and 7x- reused powder batches and the associated spatter-rich powder are presented in Fig. 3. The powder particles were highly spherical even after reusing the powder 7 times which was consistent with the observations reported in Ref. [22]. No considerable difference in morphology could be seen. A limited number of irregularly shaped and elongated particles were detected in all the powder batches (i.e., virgin, 3x- and 7x-reused) which can be due to the fabrication or powder handling.

Some particles in the reused batches showed re-solidification marks on the surface (i.e., shown by yellow arrows in the figure) which can be due to melting and re-solidification inside the chamber environment as explained in Ref [23]. Such particles were abundant in the spatter-rich powder batches and generally in the form of very large agglomerates (i.e., clusters of particles) which is typically due to the particles colliding with each other and forming agglomerates while in flight in the chamber environment [24]. The fact that only a limited number of such particles were detected in the reused batches indicates the effectiveness of the sieving process. It needs to

be noted that the PSD characterization was not conducted and the observations on morphological aspects were solely based on SEM images.
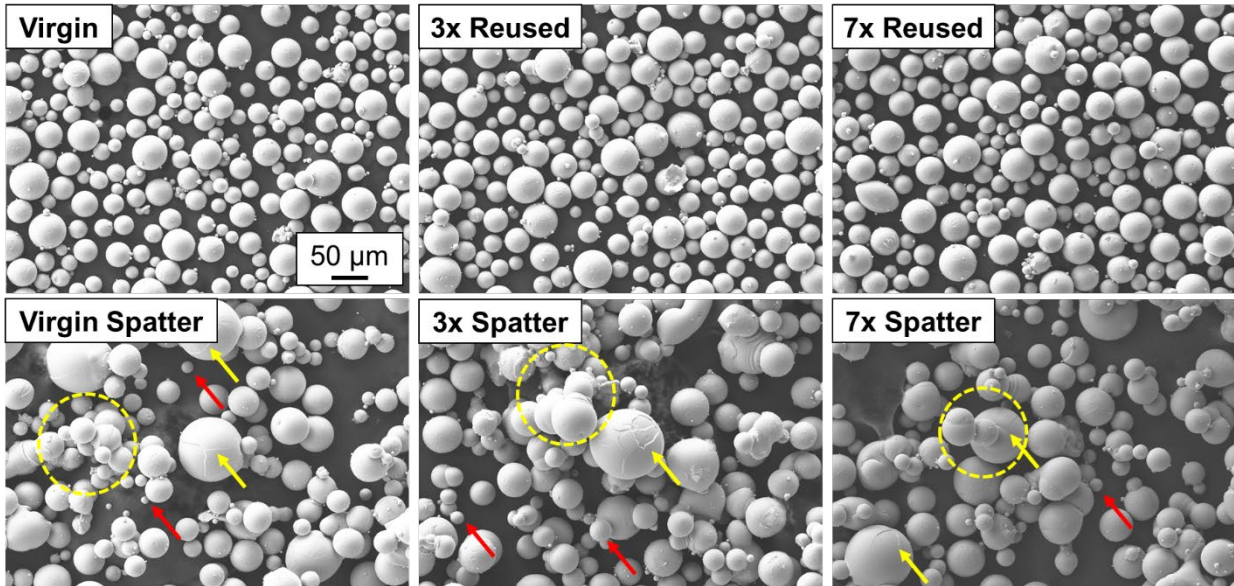

Fig. 3 Morphology of the Ti64 powder particles in virgin, 3x-reused, and 7x-reused conditions as well as the spatter powder after fabrications collected from spatter-rich regions. The scale bars in all images are 50 µm. The yellow arrows indicate the particles with remelting lines and yellow dashed circles enclose agglomerates. Red arrows also are pointed toward the smaller particles that are not affected by the fabrication process.

The majority of spatter-rich powder particles were spherical as the spatters have enough time to re-solidify in the chamber environment under argon atmosphere which can result in a very large powder size. The remaining more spherical particles with smaller sizes may be the ones unaffected by the fabrication process. Some of these particles are not removed from the chamber and can land near the spatter-rich regions in the EOS M290.

Indeed, the sieving process can remarkably contribute to the powder quality by removing such large agglomerates. These agglomerates are also reported to consist of oxide layers that can decompose during fabrication and increase the oxygen content of the parts [23,25]. In addition, the irregular shape of these particles along with the oxide film around them can decrease the heat absorptivity, giving rise to partially sintering to the side surfaces of the specimens and increase the surface roughness [17]. Lastly, some of these particles, if not properly removed, can deposit on the top surface of the specimens yielding to balling defects and disturbing the uniform powder layer distribution and more defects in the as-fabricated parts [20].

The second powder characterization step was to investigate the changes in rheological properties due to powder reuse. Powder compressibility, cohesion, and aeration energy (AE) are shown in Fig. 4. Compressibility is defined as the amount of change in density when normal stress is applied. The 7x-reused batch has the lowest compressibility as shown in Fig. 4 (a), which indicates a superior packing state in the 7x-reused powder batch and is which was consistent with Ref. [4,8,26].

Powder cohesion can represent the resistance of the powder to flow, with both being positively correlated. In L-PBF machines, the powder is distributed on the build plate via a recoater (also known as wiper or blade). Therefore, a powder batch with minimal resistance to shear stress and flow is desired. It is evident from Fig. 4 (b) that the cohesion decreased with reuse, suggesting a higher flowability and possibly a more uniform powder layer for the 7x-reused powder. The reasons why cohesion decreased with powder reuse are still under investigation. However, some possible factors can be the changes in PSD with powder reuse. As reported in [7], continuously reusing the powder may result in a decrease in finer particles as they are either used in the fabrication or ejected from the build plate during fabrication. In addition, large agglomerates were reported to decrease with the sieving process resulting in a narrower PSD. A narrower PSD is commonly associated with higher powder flowabilities [7,12,27].
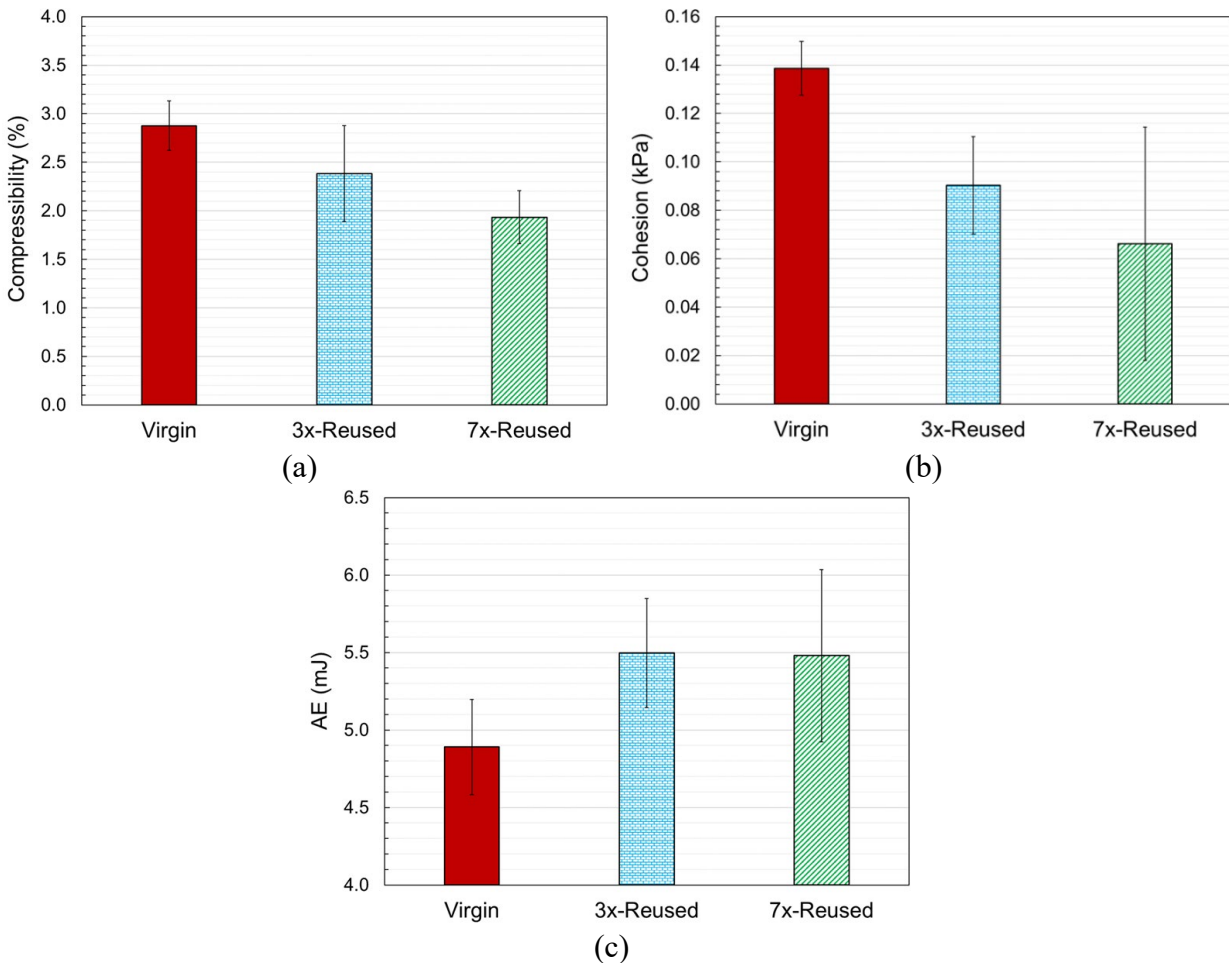

(a)

(b)

(c)

Fig. 4 A comparison of (a) compressibility, (b) cohesion, and (c) aeration energy (AE) among the virgin, 3x- and 7x-reused powder batches.

Lastly, the AE was evaluated which identifies how easily the powder can flow [28]. Therefore, powder batches with higher AE values have usually a higher tendency to agglomerate [4]. As seen in Fig. 4 (c), it seems that AE to some extent increases with powder reuse. This trend can show that there is possibly less mechanical interlocking when the virgin powder was used for

fabrication. Therefore, fewer agglomerates should have been present in this batch. The reason(s) that why agglomeration slightly increased with powder reuse is also under investigation. A possible reason, however, can be explained by spattering during fabrication. As particles eject from the build plate, they have enough time to re-solidify in the chamber environment, and in some cases, collide with each other and form larger particles [23]. Although some of these large agglomerates are successfully filtered out using the sieve, some may pass through if they are smaller than 80 µm.

Therefore, the reused batch with some of these agglomerates can show a higher AE or higher mechanical interlocking. A question might raise here that why the cohesion showed a decrease with powder reuse. This can be answered by the fact that in some conditions, agglomerates can move in the shape of "lumps" and show good flowabilities and low cohesion [28] whereas it can result in a nonuniform powder layer deposition. Therefore, the PSD characterization would be indeed needed to understand why the reused powder showed a higher AE and lower cohesion.

To evaluate the quality of the deposited powder layers during fabrication, PBD was assessed using the PBD capsules. The PBD evaluations, however, did not show any changes with powder reuse and they were between 2.63-2.65 g/cm^3 for different powder reuse iterations. However, it was found that the PBD is slightly lower in the back location (further away from the powder feedstock) for all the powder batches and it was about 2.55-2.60 g/cm^3. The location-dependent PBD values were quite interesting indicating powder segregation during spread. It is usually theorized that finer particles typically deposit near to the feedstock (i.e., front) whereas the coarser ones are pushed toward away from the feed bin (i.e., back) [5].

In addition, to understand how the powder packing state and flowability can contribute to the defect content, all XCT coupons were characterized (see Fig. 5). As shown in Fig. 5, when the virgin powder was used for fabrication, the relative densities for coupons placed near the spatter-rich regions (i.e., S and SW) were at the lowest compared with other locations. In the case of virgin powder, the maximum number of defects was detected in the SW location. When the powder was reused 7 times, the relative densities across the build plate were more consistent with less variation. Overall, it seems that the number of defects can increase by going toward the gas flow outlet. The maximum defect size for each specific location is also illustrated in Fig. 5. It needs to be specified that the maximum defect size was evaluated based on the assumption that all defects are spherical. As a result, the equivalent sphere diameter was used to compare the defect sizes.
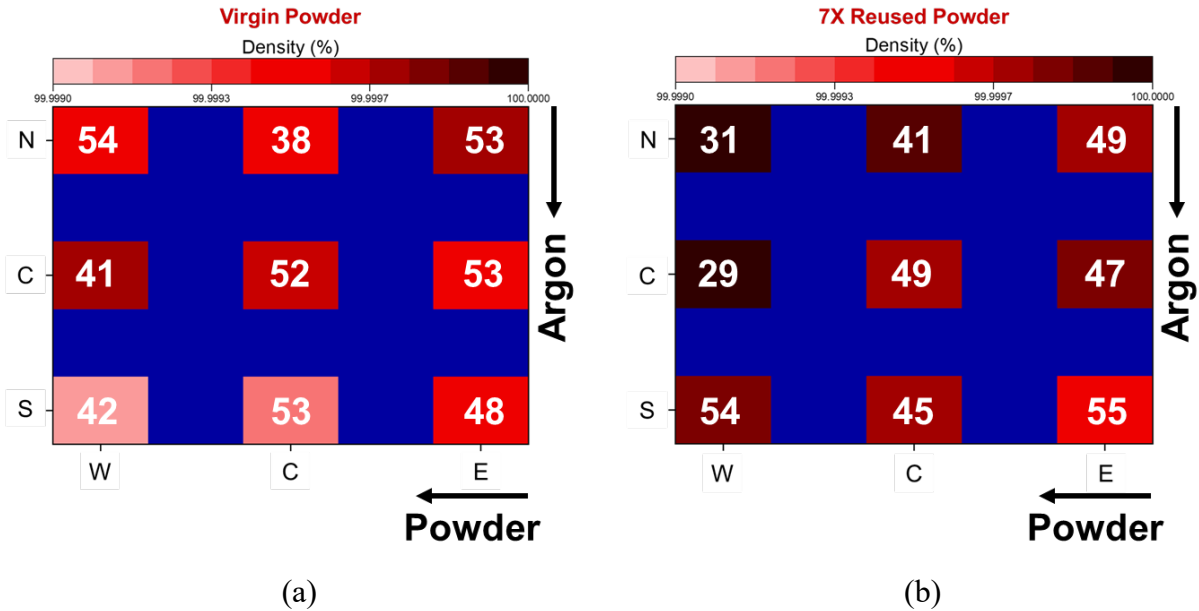
Fig. 5 Relative density of the XCT coupons in different locations for (a) virgin-print set and (b) 7x reused-print sets. The maximum defect size in each location is labeled on each box in microns.

The maximum defect size in the case of 7x-reused powder was 55 µm. This can show that the maximum defect sizes were still comparable between the first and last fabrication sets. Interestingly, a significantly large number of defects were noted in the SW locations when the virgin powder was used (almost more than 1200 defects per cm^3). Observing the maximum number of defects in this region can be attributed to some spatters landing in this zone as reported by Ref [17]. The high amount of defects in this area may verify that spatters can deteriorate the fusion and bonding between the subsequent layers as they typically have less absorptivity because of the oxide films around them.

To provide an initial understanding of whether the variation in powder characteristics resulted from the powder reuse practice as well as the build location can affect the mechanical properties, the Rockwell C hardness (HRC) value was evaluated for each condition. As seen in Fig. 6, although negligible, it seems that the HRC is increasing with continuously reusing the powder. The slightly higher HRC values of the Print 8 specimens can be possibly due to the increase in oxygen concentration with powder reuse practice which is common in Ti64 [13]. The observation on hardness was consistent with the results reported in Ref. [29] where a higher hardness was reported for the L-PBF specimens fabricated with 12-times reused powder compared with the virgin one. This increase in hardness was correlated with the oxidation of some Ti64 particles during the sieving process or removal of the parts [29]. However, thorough analyses on chemical compositions are needed to better justify this observation. In terms of location, no specific trend was noticed. Observing no correlation between the build location and HRC can be ascribed to less sensitivity of hardness tests to defect content, which is mainly affected by the powder spreadability.
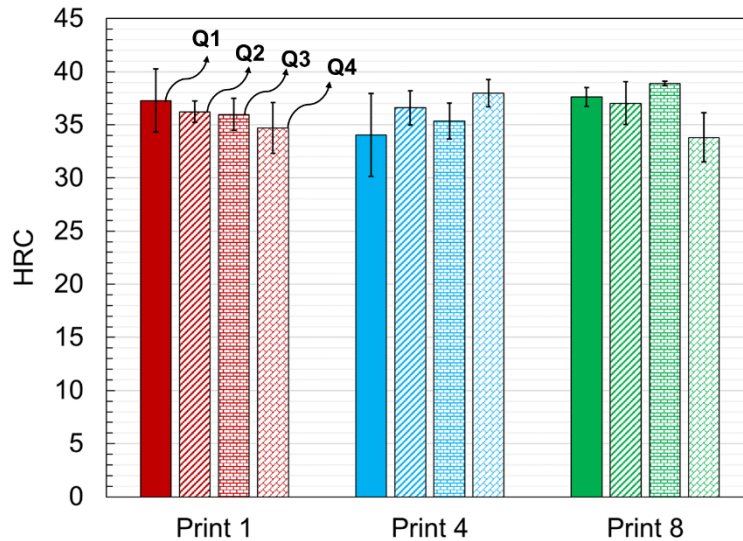
Fig. 6 The Rockwell C hardness (HRC) values for different powder reuse iterations in different locations.

Conclusions

This study investigated the effects of powder reuse as well as the build location on the powder characteristics, PBDs, defect content, and HRC values. The variations in results were explained by the changes in powder characteristics resulted from the powder reuse practice and location. The following conclusions can be drawn:

- Continuously reusing the powder resulted in a better packing state (~ 30%), flowability (~ 70%), and increased mechanical interlocking (~ 12%).
- Part density slightly increased with reusing the powder which was explained by the improved packing behavior of reused powder.
- When the virgin powder was used for fabrication, a large number of defects (more than 1200 $1/cm^3$) were noted in the SW location which was close to the inert gas outlet. This observation was ascribed to the spattering during fabrication.
- HRC values showed a slightly increasing trend with powder reuse (~ 2%) which was attributed to the possible oxygen pickup during fabrication. However, no trend was uncovered with the location of the parts.

Acknowledgment

References

[1]   A.T. Sutton, C.S. Kriewall, M.C. Leu, J.W. Newkirk, Powder characterisation techniques and effects of powder characteristics on part properties in powder-bed fusion processes,

Virtual Phys. Prototyp. 12 (2017) 3–29. doi:10.1080/17452759.2016.1250605.

[2] A.T. Sutton, C.S. Kriewall, M.C. Leu, J.W. Newkirk, Powders for Additive Manufacturing Processes: Characterization Techniques and Effects on Part Properties, Proc. 26th Annu. Int. Solid Free. Fabr. Symp. Addit. Manuf. Conf. (2016) 1004–1030. doi:10.1080/17452759.2016.1250605.

[3] J.H. Tan, W.L.E. Wong, K.W. Dalgarno, An overview of powder granulometry on feedstock and part performance in the selective laser melting process, Addit. Manuf. 18 (2017) 228–255. doi:10.1016/j.addma.2017.10.011.

[4] S.E. Brika, M. Letenneur, C.A. Dion, V. Brailovski, Influence of particle morphology and size distribution on the powder flowability and laser powder bed fusion manufacturability of Ti-6Al-4V alloy, Addit. Manuf. 31 (2020) 100929. doi:10.1016/j.addma.2019.100929.

[5] G. Jacob, C.U. Brown, A. Donmez, The Influence of Spreading Metal Powders with Different Particle Size Distributions on the Powder Bed Density in Laser-Based Powder Bed Fusion Processes, NIST Adv. Manuf. Ser. (2018) 100–17. doi:10.6028/NIST.AMS.100-17.

[6] P.E. Carrion, A. Soltani-Tehrani, S.M. Thompson, N. Shamsaei, Effect of Powder Degradation on the Fatigue Behavior of Additively Manufactured As-Built Ti-6Al-4V, Solid Free. Fabr. Proc. (2018).

[7] P.E. Carrion, A. Soltani-Tehrani, N. Phan, N. Shamsaei, Powder Recycling Effects on the Tensile and Fatigue Behavior of Additively Manufactured Ti-6Al-4V Parts, JOM. 71 (2019) 963–973. doi:10.1007/s11837-018-3248-7.

[8] A. Soltani-Tehrani, J. Pegues, N. Shamsaei, Fatigue behavior of additively manufactured 17-4 PH stainless steel: The effects of part location and powder re-use, Addit. Manuf. 36 (2020) 101398. doi:10.1016/j.addma.2020.101398.

[9] P. Dastranjy Nezhadfar, A. Soltani-Tehrani, A. Sterling, N. Tsolas, N. Shamsaei, Effects of Powder Recycling on the Mechanical Properties of Additively Manufactured Stainless Steel 17-4PH, Solid Free. Fabr. Proc. (2018) 1292–1300.

[10] R.M. German, Powder metallurgy science, 105 College Rd. E, Princeton, N. J. 08540, U. S. A, 1984.

[11] L. Cordova, T. Bor, M. de Smit, M. Campos, T. Tinga, Measuring the spreadability of pre-treated and moisturized powders for laser powder bed fusion, Addit. Manuf. 32 (2020) 101082. doi:10.1016/j.addma.2020.101082.

[12] H.P. Tang, M. Qian, N. Liu, X.Z. Zhang, G.Y. Yang, J. Wang, Effect of Powder Reuse Times on Additive Manufacturing of Ti-6Al-4V by Selective Electron Beam Melting, JOM. 67 (2015) 555–563. doi:10.1007/s11837-015-1300-4.

[13] P. Moghimian, T. Poirié, M. Habibnejad-Korayem, J.A. Zavala, J. Kroeger, F. Marion, F. Larouche, Metal Powders in Additive Manufacturing: A Review on Reusability and Recyclability of Common Titanium, Nickel and Aluminum Alloys, Addit. Manuf. (2021) 102017. doi:10.1016/j.addma.2021.102017.

[14] ASTM International, E8/E8M Standard Test Methods for Tension Testing of Metallic Materials, West Conshohocken, PA; ASTM Int. (2016). doi:https://doi.org/10.1520/E0008_E0008M-13.

[15] ASTM International, E466 Standard Practice for Conducting Force Controlled Constant Amplitude Axial Fatigue Tests of Metallic Materials, West Conshohocken, PA; ASTM Int. (2015). doi:10.1520/E0466-15.2.

[16] ASTM International, B215 Standard Practices for Sampling Metal Powders, West

Conshohocken, PA; ASTM Int. (2020). doi:https://doi.org/10.1520/B0215-15.

[17] R. Esmaeilizadeh, U. Ali, A. Keshavarzkermani, Y. Mahmoodkhani, E. Marzbanrad, E. Toyserkani, On the effect of spatter particles distribution on the quality of Hastelloy X parts made by laser powder-bed fusion additive manufacturing, J. Manuf. Process. 37 (2019) 11–20. doi:10.1016/j.jmapro.2018.11.012.

[18] J.W. Pegues, S. Shao, N. Shamsaei, N. Sanaei, A. Fatemi, D.H. Warner, P. Li, N. Phan, Fatigue of additive manufactured Ti-6Al-4V, Part I: The effects of powder feedstock, manufacturing, and post-process conditions on the resulting microstructure and defects, Int. J. Fatigue. 132 (2020) 105358. doi:10.1016/j.ijfatigue.2019.105358.

[19] S. Lee, Z. Ahmadi, J.W. Pegues, M. Mahjouri-Samani, N. Shamsaei, Laser polishing for improving fatigue performance of additive manufactured Ti-6Al-4V parts, Opt. Laser Technol. 134 (2021) 106639. doi:10.1016/j.optlastec.2020.106639.

[20] A. Soltani-Tehrani, R. Shrestha, N. Phan, M. Seifi, N. Shamsaei, Establishing Specimen Property to Part Performance Relationships for Laser Beam Powder Bed Fusion Additive Manufacturing, Int. J. Fatigue. (2021) 106384. doi:10.1016/j.ijfatigue.2021.106384.

[21] ASTM International, D7891 Standard Test Method for Shear Testing of Powders Using the Freeman Technology FT4 Powder Rheometer Shear Cell, West Conshohocken, PA; ASTM Int. (2015). doi:https://doi.org/10.1520/D7891-15.

[22] O.A. Quintana, J. Alvarez, R. Mcmillan, W. Tong, C. Tomonto, Effects of Reusing Ti-6Al-4V Powder in a Selective Laser Melting Additive System Operated in an Industrial Setting, Jom. 70 (2018) 1863–1869. doi:10.1007/s11837-018-3011-0.

[23] A.T. Sutton, C.S. Kriewall, M.C. Leu, J.W. Newkirk, B. Brown, Characterization of laser spatter and condensate generated during the selective laser melting of 304L stainless steel powder, Addit. Manuf. 31 (2020) 100904. doi:10.1016/j.addma.2019.100904.

[24] E. Santecchia, S. Spigarelli, M. Cabibbo, Material reuse in laser powder bed fusion: Side effects of the laser—metal powder interaction, Metals (Basel). 10 (2020) 1–21. doi:10.3390/met10030341.

[25] M. Simonelli, C. Tuck, N.T. Aboulkhair, I. Maskery, I. Ashcroft, R.D. Wildman, R. Hague, A Study on the Laser Spatter and the Oxidation Reactions During Selective Laser Melting of 316L Stainless Steel, Al-Si10-Mg, and Ti-6Al-4V, Metall. Mater. Trans. A Phys. Metall. Mater. Sci. 46 (2015) 3842–3851. doi:10.1007/s11661-015-2882-8.

[26] S.E. Brika, V. Brailovski, Influence of Powder Particle Morphology on the Static and Fatigue Properties of Laser Powder Bed-Fused Ti-6Al-4V Components, J. Manuf. Mater. Process. 4 (2020) 107. doi:10.3390/jmmp4040107.

[27] A. Soltani-Tehrani, M.S. Yasin, S. Shao, M. Haghshenas, N. Shamsaei, Effects of Powder Particle Size on Fatigue Performance of Laser Powder-Bed Fused Ti-6Al-4V, in: Fatigue Des. 2021, 9th Ed. Int. Conf. Fatigue Des., 2021.

[28] Freeman Technology, FT4 Powder Rheometer - Summary of Methodologies, (2008).

[29] V. Seyda, N. Kaufmann, C. Emmelmann, Investigation of Aging Processes of Ti-6Al-4V Powder Material in Laser Melting, Phys. Procedia. 39 (2012) 425–431. doi:10.1016/j.phpro.2012.10.057.